IEEE Access
Multidisciplinary : Rapid Review : Open Access Journal

Received March 8, 2019, accepted March 22, 2019, date of publication April 2, 2019, date of current version April 19, 2019.

Digital Object Identifier 10.1109/ACCESS.2019.2908819

Emotion-Specific Facial Activation Maps Based on Infrared Thermal Image Sequences

BO-LIN JIAN[1], CHIEH-LI CHEN[2], (Member, IEEE), MIN-WEI HUANG[3], AND HER-TERNG YAU[1], (Senior Member, IEEE)

[1]Department of Electrical Engineering, National Chin-Yi University of Technology, Taichung, Taiwan
[2]Department of Aeronautics and Astronautics, National Cheng Kung University, Tainan, Taiwan
[3]Department of Psychiatry, Chiayi Branch, Taichung Veterans General Hospital, Chiayi, Taiwan

Corresponding author: Her-Terng Yau (pan1012@ms52.hinet.net)

This work was supported by the National Science Council of the Republic of China, Taiwan, under Contract MOST 107-2218-E-167-001.

ABSTRACT Research on emotion recognition has recently started to gain increased attention. Inner emotions or thought activity can be determined by analyzing facial expression, behavioral responses, audio, and physiological signals. Facial expression is now recognized as an important form of non-verbal interaction. In this paper, emotion-specific activation maps were constructed to establish infrared thermal facial image sequences as an alternative approach to the determination of the correlation between emotional triggers and changes in facial temperature. During the testing process, data stored in the International Affective Picture System were used to create emotional clips that triggered three different types of emotion in the subjects, and their infrared thermal facial image sequences were simultaneously recorded. For processing, an image calibration protocol was first employed to reduce the variance produced by irregular micro-shifts in the faces of the subjects, followed by independent component analysis and statistical analysis protocols to create the facial emotional activation maps. The test results showed that the problem of selecting local regions when analyzing frame temperature had been resolved. The emotion-specific facial activation maps provide visualized results that facilitate the observation and understanding of information.

INDEX TERMS Thermal image, independent component analysis, periorbital region, activation map.

I. INTRODUCTION

In recent years, numerous investigations of observable expression recognition have been made [1]–[3]. However, involuntary happiness, anger, sadness, or other emotion can be concealed, easily causing misinterpretation of emotions. In addition, expression recognition may also be influenced by environmental lighting and facial posture [4], which can also cause errors in system recognition. In response, studies were started using infrared thermal images to reduce the influence of lighting on emotion response recognition [5], [6]. Methods to observe temperature changes in facial regions under different emotional stimuli have been proposed, and the results of applying these have been reported. Pollina *et al.* [7] reported a polygraph study based on temperature changes in the orbital region, and the results showed that polygraphs and temperature changes were related. The researchers also asserted that temperature changes between the left and right sides of the face are different, highlighting that temperature changes of the periorbital region are correlated to psychological status. Nhan and Chau [8], [9] used infrared thermal facial image data to elucidate the feasibility of classifying affective states. The researchers contended that the continuous temperature signals from the nasal and periorbital region exhibit significant temperature changes, rendering these signals ineffective for determining a correlation between the temperature results of facial regions and emotions. Shastri *et al.* [10] analyzed wavelet energy and found an increased significance in the correlation between the temperature of the periorbital region and emotions upon audio stimuli. Gane *et al.* [11] analyzed temperature changes elicited in the periorbital region upon an auditory startle stimulus. The results showed no significant correlation between the auditory startle stimulus and the periorbital region. The researchers suspected that these results were attributed to the fact that the audio stimuli did not startle the subjects. A summary of previous research results shows a relatively high correlation between emotions and temperature in the

The associate editor coordinating the review of this manuscript and approving it for publication was Kathiravan Srinivasan.

periorbital [12]–[14] and nasal regions [14], [15]. The results confirmed subtle changes in the facial temperature when specific emotions were successfully triggered. Jian *et al.* [16] analyzed the facial temperature in five locations of moderately ill and significantly ill schizophrenia patients. The successful response was significantly different between the two groups. However, these studies used methods to determine sequential changes in the average temperature of specific facial regions to elucidate the correlation between facial temperature and emotion. However, there was no completely successful solution to the problem. When analyzing sequence imaging, the problem of image segmentation and registration will be faced. Many researchers adopt different theoretical bases to solve this type of problem. After discussing the literature analysis [17], image calibration can be divided into two methods: feature and area. The feature-based image calibration is not applicable for occasion with high nonlinearity differences [18]. Hence, this study adopted the affine parameter regional calibration method [19]. In addition, Chen and Jian [19] have proven the sound effectiveness of solving image calibration problems through the 2-stage genetic algorithm method, while the problem of image segmentation is resolved. Therefore, this study adopted the process [19] to carry out image registration, thereby resolving the alignment problem between images.

To establish emotional activation maps for local and nonlocal facial regions, independent component analysis (ICA) was used in this study to resolve the relevant problems. ICA is a method that distinguishes primitive signals from mixed signals to determine linearity. It has become a practical tool for the identification of hidden information [20] and has been successfully incorporated into a number of imaging and image processing fields [21]–[23]. For example, ICA was incorporated into functional magnetic resonance imaging (fMRI) to effectively display the differences in the responses of the lower region of the brain to different stimuli [24]. In this study, fast fixed-point algorithms were employed for the ICA calculations, which calculate non-Gaussian maxima via fixed-point iterations. This method enhances the speed and accuracy of ICA algorithmic calculations [25] and improves the robustness and stability of the mathematical methods employed for probing mutually independent components. Subsequently, fast fixed-point algorithms have been successfully applied to fMRI to comprehensively analyze activation maps [26]–[28].

Emotional responses triggered by external stimuli are affected by subjective factors. Thus, the subjective judgements of individuals also reflect their existing physical and psychological condition. Previous studies on emotion triggering have often employed different methods to trigger emotions. Gross and Livenson [29] used the stimuli of various video sequences to trigger the emotional responses of subjects. Lang *et al.* [30] used images to stimulate the emotional level of subjects and objectively established an assessment standard for visual complexity and emotional responses. Palomba *et al.* [31] used video segments with threatening content and surgical procedures to trigger emotional responses in subjects. Kim *et al.* [32] adopted numerous environmental factors, such as lighting color and music, to create different environments, which were used to trigger emotion. New methods have been adopted more recently, but lack objective trigger-strength standards and diversity. The International Affective Picture System (http://csea.phhp.ufl.edu/Media.html) developed by Lang et al was used in this study [30]. The IAPS system comprises a database of over 1,000 full color images, and is currently the most up-to-date. Subsequently, it has received positive reviews for effectiveness in triggering emotion in subjects in many studies [33]–[36].

II. METHODS

A. THERMAL IMAGE DATA ACQUISITION

Because the testing environment and human factors can cause statistical error, the control of any ambient temperature changes was necessary. In this study, the digital infrared thermal image system (DITIS) used was the Spectrum series 9000-MB (United Integrated Service Co Ltd). The infrared thermal face image collection area used was 320×240 pixels for the temperature data matrix, at a sampling frequency of 2 fps. The machine specification of noise equivalent temperature difference was 0.07°C and the temperature measurement range was 10°C to 40°C. During data collection, subjects who were on long-term medication or had fever or influenza, were excluded. A total of five subjects participated in this study. Prior to data collection, the subjects were instructed to watch a black screen for 5 minutes to ensure that they had reached thermal equilibrium. Then, a 5 second verbal reminder was issued to notify the subjects that the test was about to begin. During data collection, no other persons were allowed to enter the room to maintain the room temperature between 26°C and 28°C and to avoid the generation of strong heat convection. The test area was surrounded and insulated by three layers of dark fabric to minimize reflected heat radiation. To protect the rights and ensure the safety and comfort of the subjects their heads were not restrained in any way during the experiments.

B. STIMULI AND PARADIGM

To ensure that the 45 IAPS images resulted in differences of arousal and valence, the participants included 100 subjects 48 males (mean age of 35.94 ± 12.38) and 52 females (mean age of 37.45 ± 14.14) who were all raised in Taiwan. The subjects all completed a questionnaire and the results showed parallel-type reliability. Figure 1 shows the 45 images classified into three different emotions, designated as HVLA (High Valence Low Arousal), LVLA (Low Valence Low Arousal) and LVHA (Low Valence High Arousal). Subsequently, the selected IAPS images were edited into an emotion-stimulating video. The video was 225 seconds long and aimed at stimulating four emotions, which included HVLA, LVLA, LVHA, and Rest. The display sequence and times of the images are shown in Figure 2.

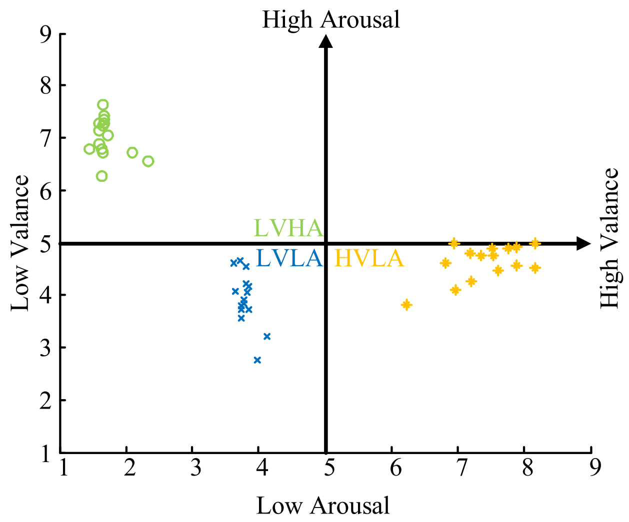

FIGURE 1. 45 IAPS images where emotional assessments can be accounted for by the two dimensions of valence and arousal as three different emotions HVLA, LVLA and LVHA.

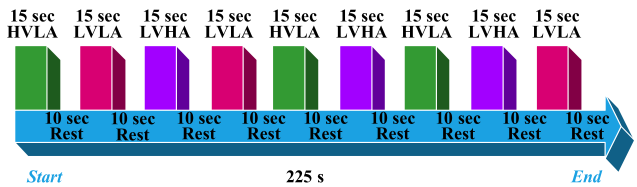

FIGURE 2. The serial reaction time series of the IAPS images. The emotion-stimulating time for each block was 15 sec (five images were displayed, each for 3 sec) and the rest time was 10 sec for each.

C. INFRARED THERMAL IMAGE SEQUENCES PROCESSING

Infrared thermal facial image sequence data were collected to develop a method for analyzing the relationship between facial temperature and emotion. Each sequence image processed by image registration determined the correlation between the average temperature-sequence changes in the facial regions and the emotional stimulus response via both activation maps and the temperature of each facial region. The overall research framework is shown in Figure 3.

D. IMAGE REGISTRATION

To ensure the subjects remained comfortable while the infrared thermal image data sequences of the faces were collected their heads were not restrained in any way. Unintentional head movement caused some issues and made subsequent analysis more difficult. Therefore, affine registration was used to reduce deviations resulting from head movement and to enhance the validity of the facial correlation analysis. During the registration process, a fixed image for registration was produced by locating the centroid in the eye region. Image translations and rotations were also used. Subsequently, the two-stage genetic algorithm proposed by Chen and Jian [19] was used to automatically complete the affine registration of the thermal sequential imaging. This method effectively reduced overlay error before and after image registration.

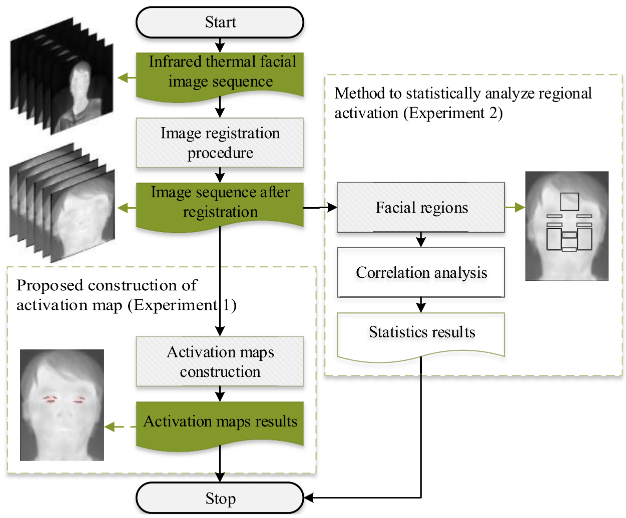

FIGURE 3. Research infrastructure for activation maps and regional activation. After the registration procedure, the infrared thermal facial images for two experiments: One was to construct activation maps and the other for regional activation.

E. CONSTRUCTION OF THE ACTIVATION MAPS

To observe significant changes in the facial temperatures of the subjects during emotion stimulation, emotional activation maps were constructed to create infrared thermal facial image sequences as follows:

1. Infrared thermal facial image sequence data. $\mathbf{FIs} \leftarrow \{\mathbf{FI_1}, \mathbf{FI_2}, \ldots, \mathbf{FI_S}\}$, $\mathbf{FI}$ is a facial image of 320×240 matrix, s is a 450 frame sequence.
2. Eliminate temperature noise of non-ROIs using imaging masking. $\mathbf{MIs} \leftarrow \{\mathbf{MI_1}, \mathbf{MI_2}, \ldots\mathbf{MI_s}\}$, $\mathbf{MI} = \mathbf{FI\&ImageMask}$, **ImageMask** is a binary image with 0 and 1 (0 is outside the mask; 1 is inside the mask of interest), and is the AND operation.
3. Reshape the **MIs** matrices into **x** matrices (matrix size of 450×76800).
4. The pseudocode was:

$s = 450$; $MI\_RowLength = 240$;
$MI\_ColumnLength = 320$;
for $Frame = 1 : s$
  $Counter = 1$;
  for $i = 1 : MI\_RowLength$
    for $j = 1 : MI\_ColumnLength$
      $\mathbf{x}(\text{Frame, Counter}) = \mathbf{MI.SubMatrix}.\mathrm{s}(i, j)$;
      $Counter = Counter + 1$;
    end
  end
end

5. Use FastICA to determine the independent statistics shown in Table 1. The matrix decomposition and arrangement is shown in Figure 4, where **x** represents the matrix arranged by the infrared thermal images at

TABLE 1. FastICA algorithm for estimating several ICs with deflationary orthogonalization.

Inputs: matrix $\mathbf{x}$.
Outputs: mixing matrix $\hat{\mathbf{w}}^{-1}$ and independent components $\mathbf{ICs}$.

1. Centerline the data to make its mean zero. $\mathbf{x} \leftarrow \mathbf{x} - E\{\mathbf{x}\}$
2. To obtain $\mathbf{z}$. we whiten the data, $\mathbf{z} = \mathbf{V}\mathbf{x} = \mathbf{D}^{-1/2}\mathbf{E}^{T}\mathbf{x}$, where $\mathbf{D}$ is the diagonal matrix of the eigenvalues, $\mathbf{E}$ is the matrix whose columns are the unit norm eigenvectors of covariance of the $\mathbf{x}$ matrix.
3. Pick m to estimate the number of $\mathbf{ICs}$. Set counter $p \leftarrow 1$.
4. Let $\mathbf{w}_{\mathbf{p}}$ be an initial value of the unit norm. (randomly)
5. Derivation of the fixed-point iteration in FastICA: $\mathbf{w}_{\mathbf{p}} \leftarrow E\{\mathbf{z} \times g(\mathbf{w}_{\mathbf{p}}^{T} \times \mathbf{z})\} - E\{g'(\mathbf{w}_{\mathbf{p}}^{T} \times \mathbf{z})\} \times \mathbf{w}_{\mathbf{p}}$. We choose a nonlinearity, $g(h) = g \times \exp(-h^2/2)$, $g'(h) = (1-h^2) \times \exp(-h^2/2)$.
6. Perform the following orthogonalization algorithms using the Gram–Schmidt processing method: $\mathbf{w}_{\mathbf{p}} \leftarrow \mathbf{w}_{\mathbf{p}} - \sum_{j=1}^{p-1} (\mathbf{w}_{\mathbf{p}}^{T}\mathbf{w}_{\mathbf{j}})\mathbf{w}_{\mathbf{j}}$.
7. Let $\mathbf{w}_{\mathbf{p}} \leftarrow \mathbf{w}_{\mathbf{p}} / \|\mathbf{w}_{\mathbf{p}}\|$.
8. Set $p \leftarrow p+1$. If $p \leq m$, go back to step 4.
9. $\hat{\mathbf{w}} = \mathbf{w}^{T} \times \mathbf{V}$, $\mathbf{w} = [\mathbf{w}_1\ \mathbf{w}_2 \ldots \mathbf{w}_{\mathbf{p}}]$.
10. $\mathbf{ICs} = \hat{\mathbf{w}} \times \mathbf{x} \Rightarrow \mathbf{x} = \hat{\mathbf{w}}^{-1} \times \mathbf{ICs}$. $\hat{\mathbf{w}}^{-1}$ is mixing matrix, $\mathbf{ICs}$ is independent components.

Expectations were estimated as sample averages.

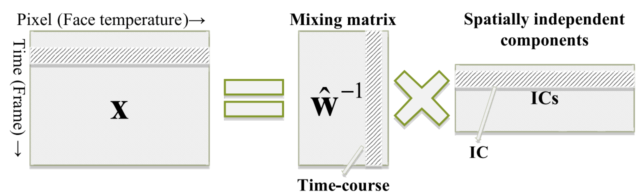

FIGURE 4. Schematic of the data representation and spatial decomposition performed by the spatial ICA on the thermal imaging data.

different times. By decomposing the matrix, the product of the mixing matrix and the spatially independent components (ICs) can be obtained, and the size of the mixing matrix was 450 × 450. Each row represents independent time course estimates. The time courses correspond to the spatial ICs in each row. Subsequently, each IC contains spatial information. Thus, the spatial information regions can be identified only by observing the time course information that corresponds to the ICs.

6. Use one-way analysis of variance to determine the p-value of the time courses and the serial reaction time task and find the minimum p-value's time-course that corresponds to the independent component (IC).
7. Use the Z-score filter (threshold = 2) to highlight the facial response regions, thereby eliminating the influence of noise on the spatial ICs.
8. The Z-score was $\mathbf{Zscore_{OneDim}}$=($\mathbf{MaxSignIC}$ − Avg($\mathbf{MaxSignIC}$)/SD). $\mathbf{MaxSignIC}$ is the maximum significant $\mathbf{ICs}$, Avg($\mathbf{MaxSignIC}$) is the average of, and SD is $\mathbf{MaxSignIC}$ standard deviation of $\mathbf{MaxSignIC}$.
9. Finally, employ a matrix reshape to return the one-dimensional $\mathbf{Zscore_{OneDim}}$ to a two-dimensional $\mathbf{Zscore_{OneDim}}$ matrix. The matrix is superimposed onto the original facial image to produce an activation map that highlights significant facial response changes in emotion.
10. The pseudocode for matrix reshape to two-dimensions is:

```
MI_RowLength = 240; MI_ColumnLength = 320;
Counter = 1;
for i = 1 : MI_RowLength
  for j = 1 : MI_ColumnLength
    Zscore.Two(i, j) = Zscore.One(Counter);
    Counter = Counter + 1;
  end
end
```

F. FACIAL REGIONS

Faces were divided into nine regions, including the central regions (forehead, tip of the nose and mouth) and left and right side regions (eye upper, eye lower and cheek). The facial image of subject 1 was used as the region for calculating the temperature, as shown in Figure 5(a). The choice of facial area was based on previous relevant research articles and experience [8], [9]. We calculated each of the nine regions according to serial reaction time tasks and then performed a correlation analysis of the average temperature and emotional stimulation.

III. EXPERIMENTAL RESULTS AND DISCUSSION

In this study emotional activation maps were used to establish infrared thermal facial image sequences and analyze the facial temperature regions to calculate significance in different facial regions. The average temperature of the regions in each infrared thermal image could be determined based on the definitions established for each facial region. In this context, we selected the facial regions of subject 1, as shown in Figure 5 (a). The average temperatures of the regions in each image were recorded to obtain signals for the changes in their average temperature over time, as illustrated in Figure 5 (b). Finally, a correlation analysis was performed on the serial reaction time data. The results showed the level of correlation between the serial reaction time task for the temperatures of the different facial regions and the different emotions. Using this method to investigate the correlation between emotions and facial region temperatures increased our understanding, but also posed two challenges. The first was non-stationary facial temperature signals. In the case of subject 1 in Figure 5 (b), the various signals gradually trended upwards as the frame number increased. The results

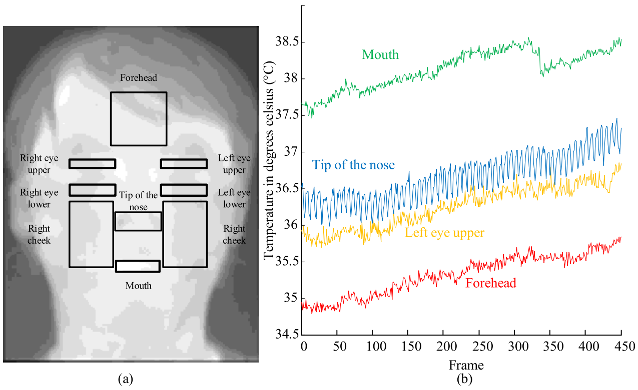

FIGURE 5. Regional statistical analysis: (a) Schematic of a face divided into nine regions with divisions based on central, left and right sides. (b) Signal diagram of the changes in temperature of the facial regions of subject 1 as a function of time.

TABLE 2. The result of activation maps in different types of emotional stimuli.

Subjects (Sex/Age) / Different Types of Emotions	Sub. 1 (Male/27)	Sub. 2 (Female/30)	Sub. 3 (Female/27)	Sub. 4 (Female/46)	Sub. 5 (Male/58)
All types	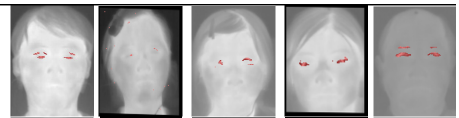				
Type1 HVLA	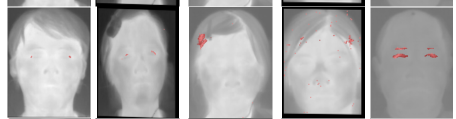				
Type2 LVLA	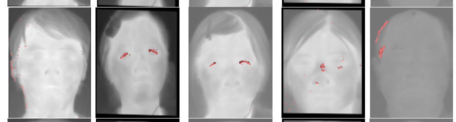				
Type3 LVHA	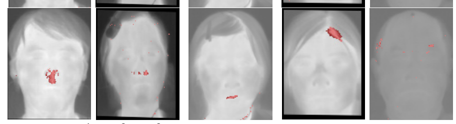				
	Imposed on face from z-score				

failed to present a fixed pattern and indicated considerable fluctuation and changes in temperature signals over a short period. This phenomenon increased the difficulty of analysis. Generally, these signals cannot guarantee that the physiological temperature signals induced by the IAPS are synchronous with the serial reaction time task. Therefore, this study adopted a p-value for the one-way analysis of variance, commonly used in statistical calculations, to determine the correlation between the temperatures in the facial regions and the serial reaction time task and reduce the influence of non-stationary temperature signals and unsynchronized psychologically induced factors. The second challenge was the requirement to predetermine the facial regions prior to calculating correlation. During the analysis process, the facial region correlations could not be immediately determined. To resolve this issue, we reviewed solutions used in various fields and decided to use activation maps to analyze the two-dimensional time sequence data. Activation maps were established based on the fMRI calculation method proposed by Calhoun and Adali [37]. This algorithm effectively removed the influence that facial region selection standards and non-stationary facial temperature signals have on the statistical results when calculating facial temperature sequences [8], [9]. The signals in the infrared thermal facial image sequences contained a large amount of unimportant background noise. Subsequently, the function of the FastICA was primarily to identify the original statistically independent primitive signals from the mixed data. In this study four emotional activation maps were highlighted using a serial reaction time task to visualize and quantify the results. However, 450 spatial ICs remained and it was not possible to analyze them. Previous studies only examined the results from corresponding serial reaction time tasks. Other emotions may exist in these remaining spatial ICs. In addition to the three types of emotions (i.e., HVLA, LVLA and LVHA) that may be triggered by the IAPS images, the subjects may also simultaneously generate other emotions. These unknown emotions may be concealed in the 450 spatial ICs. These unknown emotions certainly include interactive influences between emotions. The results were similar to the results of the activation maps generated from all emotions tabulated in Table 2, which showed that the decomposition of signals using FastICA produced linear and independent primitive signals. However, different emotions were uncovered once a linear and independent primitive signal was decomposed. All subjects exhibited significant temperature changes in the periorbital region, and the different emotions were integrated and expressed through physiological signals. Thus, in terms of a single linear and independent primitive signal or time course, the response time contains the integration of all emotions. In terms of a physiological mechanism, the response is an integrated one. However, the response becomes an independent signal once decomposed through the ICA. Thus, different emotion serial reaction time tasks and tests can be designed using this method to investigate the physiological signals of the face and determine interesting stimuli signals and physiological results. The procedures established in this study can assist future studies regarding temperature changes present in infrared thermal facial image sequences caused by emotional or other stimuli. This is similar to the generalization of ICA techniques in the field of fMRI [38], [39] and shows the proposed method to be extremely reliable. The activation map results in Table 2 show an increased overall temperature change in the periorbital region, regardless of the emotions of the subjects. We believe that this temperature change is associated with soft connective and adipose tissue, and the abundance of micro-vessels surrounding the periorbital region. Thus, temperature can be transferred through the micro-vessels to express physiological signals. This temperature change may also be associated with muscle movement in the periorbital region. When an LVHA emotion was stimulated in a subject, involuntary breathing and temperature changes took place and the mouth opened and closed slightly.

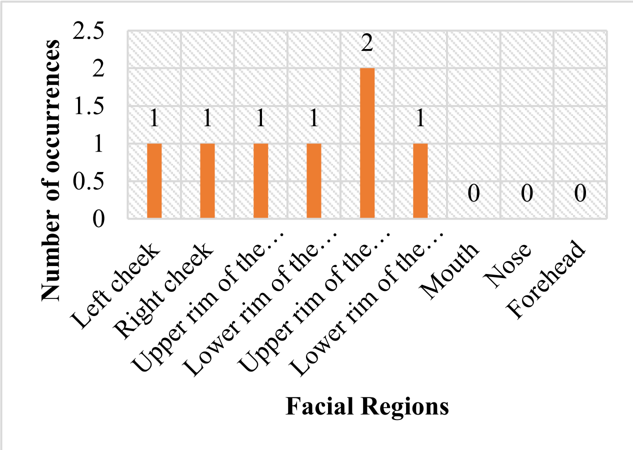

FIGURE 6. Number of occurrences ($p < 0.01$) of emotional responses at each facial region. The results show that the cheek and eye regions correlate with emotions.

These movements increased the temperature change in the periorbital and nose regions. Because we did not retrain the head during the testing process, we were unable to calibrate excessive head movement or the movement of hair, even when using genetic algorithms in two stages [19], consequently this caused errors. For these reasons, we observed slight temperature changes on the edges of the head and hair images.

The results of the proposed analysis procedures were compared with those of the facial regions analysis and Figure 6 shows the number of significant correlations ($p < 0.01$) in the different regions. In terms of the distribution of the number of significant correlations in the different regions, the periorbital region achieved the highest proportion (25%), followed by the cheek, mouth, nose, and forehead regions (20%, 0%, 0%, and 0%, respectively). Both analysis methods indicated that the periorbital region achieved the highest significance, which is consistent with the results of extant studies [7], [12], [13] and the emotional activation maps constructed in this study. However, the correlation results of the region temperature sequences only showed response changes in local regions of the face. In this study, calibration was completed during the establishment of the procedure. Then, FastICA was employed to process the infrared thermal facial image sequences and obtain the activation maps that corresponded to facial emotions. This method enabled us to directly observe significant micro facial responses upon emotional stimuli and was not limited to application to specific facial regions. This is an analytical method for emotion response research that has an intuitive approach.

IV. CONCLUSION

This study established a set of procedures to analyze the correlation between infrared thermal facial image sequences and emotional stimuli. Significance analysis methods commonly used in the field of fMRI were examined, and the concepts were incorporated in the emotional correlation of the infrared thermal facial image sequence data to visualize relevant images. First, image registration was employed to align each sequence image, and reduce the variance created by the irregular micro-movements of the subjects. Sequence images were then cross-verified to construct emotional activation maps and two calculations of the average temperatures in the facial regions were recorded. The test results highlighted the increased significance of the periorbital region, which is consistent with the results of other studies. This confirmed the feasibility of the proposed method and confirmed that activation maps can be constructed without predetermining local facial regions, thereby resolving the difficulties that non-stationary temperature changes have on data analysis. Moreover, the proposed method improved data visualization, facilitating subsequent analysis of the correlation between emotions and facial temperature.

REFERENCES

[1] S. Ulukaya and C. E. Erdem, "Gaussian mixture model based estimation of the neutral face shape for emotion recognition," *Digit. Signal Process.*, vol. 32, pp. 11–23, Sep. 2014.
[2] A. Azazi, S. L. Lutfi, I. Venkat, and F. Fernández-Martínez, "Towards a robust affect recognition: Automatic facial expression recognition in 3D faces," *Expert Syst. Appl.*, vol. 42, no. 6, pp. 3056–3066, 2015.
[3] S. H. Abdurrahim, S. A. Samad, and A. B. Huddin, "Review on the effects of age, gender, and race demographics on automatic face recognition," *Vis. Comput.*, vol. 34, no. 11, pp. 1617–1630, Nov. 2018.
[4] M. P. Beham and S. M. M. Roomi, "A review of face recognition methods," *Int. J. Pattern Recognit. Artif. Intell.*, vol. 27, no. 4, Jun. 2013, Art. no. 1356005.
[5] E. F. J. Ring and K. Ammer, "Infrared thermal imaging in medicine," *Physiol. Meas.*, vol. 33, no. 3, pp. R33–R46, Feb. 2012.
[6] A. Di Giacinto, M. Brunetti, G. Sepede, A. Ferretti, and A. Merla, "Thermal signature of fear conditioning in mild post traumatic stress disorder," *Neuroscience*, vol. 266, pp. 216–233, Apr. 2014.
[7] D. A. Pollina *et al.*, "Facial skin surface temperature changes during a 'concealed information' test," *Ann. Biomed. Eng.*, vol. 34, no. 7, pp. 1182–1189, Jul. 2006.
[8] B. R. Nhan and T. Chau, "Infrared thermal imaging as a physiological access pathway: A study of the baseline characteristics of facial skin temperatures," *Physiol. Meas.*, vol. 30, no. 4, pp. N23–N35, Apr. 2009.
[9] B. R. Nhan and T. Chau, "Classifying affective states using thermal infrared imaging of the human face," *IEEE Trans. Biomed. Eng.*, vol. 57, no. 4, pp. 979–987, Apr. 2010.
[10] D. Shastri, A. Merla, P. Tsiamyrtzis, and I. Pavlidis, "Imaging facial signs of neurophysiological responses," *IEEE Trans. Biomed. Eng.*, vol. 56, no. 2, pp. 477–484, Feb. 2009.
[11] L. Gane, S. Power, A. Kushki, and T. Chau, "Thermal imaging of the periorbital regions during the presentation of an auditory startle stimulus," *PLoS ONE*, vol. 6, no. 11, Nov. 2011, Art. no. e27268.
[12] A. Perry, H. Aviezer, P. Goldstein, S. Palgi, E. Klein, and S. G. Shamay-Tsoory, "Face or body? Oxytocin improves perception of emotions from facial expressions in incongruent emotional body context," *Psychoneuroendocrinology*, vol. 38, no. 11, pp. 2820–2825, Nov. 2013.
[13] A. Lischke, C. Berger, K. Prehn, M. Heinrichs, S. C. Herpertz, and G. Domes, "Intranasal oxytocin enhances emotion recognition from dynamic facial expressions and leaves eye-gaze unaffected," *Psychoneuroendocrinology*, vol. 37, no. 4, pp. 475–481, Apr. 2012.
[14] M. S. Panasiti, D. Cardone, E. F. Pavone, A. Mancini, A. Merla, and S. M. Aglioti, "Thermal signatures of voluntary deception in ecological conditions," *Sci. Rep.*, vol. 6, Oct. 2016, Art. no. 35174.
[15] B. Manini, D. Cardone, S. J. H. Ebisch, D. Bafunno, T. Aureli, and A. Merla, "Mom feels what her child feels: Thermal signatures of vicarious autonomic response while watching children in a stressful situation," *Front Hum. Neurosci.*, vol. 7, p. 299, Jun. 2013.
[16] B. L. Jian, C. L. Chen, W. L. Chu, and M. W. Huang, "The facial expression of schizophrenic patients applied with infrared thermal facial image sequence," *BMC Psychiatry*, vol. 17, no. 1, p. 229, Jun. 2017.

[17] M. A. Viergever, J. B. A. Maintz, S. Klein, K. Murphy, M. Staring, and J. P. W. Pluim, "A survey of medical image registration–under review," *Med. Image Anal.*, vol. 33, pp. 140–144, Oct. 2016.
[18] C. L. Tsai, C.-Y. Li, G. Yang, and K.-S. Lin, "The edge-driven dual-bootstrap iterative closest point algorithm for registration of multimodal fluorescein angiogram sequence," *IEEE Trans. Med. Imag.*, vol. 29, no. 3, pp. 636–649, Mar. 2010.
[19] C.-L. Chen and B.-L. Jian, "Infrared thermal facial image sequence registration analysis and verification," *Infr. Phys. Technol.*, vol. 69, pp. 1–6, Mar. 2015.
[20] A. Hyvãrinen and E. Oja, "Independent component analysis: Algorithms and applications," *Neural Netw.*, vol. 13, nos. 4–5, pp. 411–430, Jun. 2000.
[21] K. Chen *et al.*, "Characterization of the image-derived carotid artery input function using independent component analysis for the quantitation of [18F] fluorodeoxyglucose positron emission tomography images," *Phys. Med. Biol.*, vol. 52, no. 23, pp. 7055–7071, Dec. 2007.
[22] K.-H. Su, J.-S. Lee, J.-H. Li, Y.-W. Yang, R.-S. Liu, and J.-C. Chen, "Partial volume correction of the micro PET blood input function using ensemble learning independent component analysis," *Phys. Med. Biol.*, vol. 54, no. 6, pp. 1823–1846, Mar. 2009.
[23] R.-B. Chen, Y. Chen, and W. K. Härdle, "TVICA—Time varying independent component analysis and its application to financial data," *Comput. Statist. Data Anal.*, vol. 74, pp. 95–109, Jun. 2014.
[24] C. F. Beckmann, "Modelling with independent components," *NeuroImage*, vol. 62, no. 2, pp. 891–901, 2012.
[25] A. Hyvarinen, "Fast and robust fixed-point algorithms for independent component analysis," *IEEE Trans. Neural Netw.*, vol. 10, no. 3, pp. 626–634, May 1999.
[26] K. Suzuki, T. Kiryu, and T. Nakada, "Fast and precise independent component analysis for high field fMRI time series tailored using prior information on spatiotemporal structure," *Hum. Brain Mapping*, vol. 15, no. 1, pp. 54–66, Jan. 2002.
[27] H. Shen, M. Kleinsteuber, and K. Huper, "Local convergence analysis of fastICA and related algorithms," *IEEE Trans. Neural Netw.*, vol. 19, no. 6, pp. 1022–1032, Jun. 2008.
[28] Z. Long, Z. Wang, J. Zhang, X. Zhao, and L. Yao, "Temporally constrained ICA with threshold and its application to fMRI data," *BMC Med. Imag.*, vol. 19, no. 1, Jan. 2019, Art. no. 6.
[29] J. J. Gross and R. W. Levenson, "Emotion elicitation using films," *Cogn. Emotion*, vol. 9, no. 1, pp. 87–108, 1995.
[30] P. J. Lang, R. F. Simons, M. Balaban, and R. Simons, *Attention and Orienting: Sensory and Motivational Processes*. Psychology Press, 2013.
[31] D. Palomba, M. Sarlo, A. Angrilli, A. Mini, and L. Stegagno, "Cardiac responses associated with affective processing of unpleasant film stimuli," *Int. J. Psychophysiol.*, vol. 36, no. 1, pp. 45–57, Apr. 2000.
[32] K. H. Kim, S. W. Bang, and S. R. Kim, "Emotion recognition system using short-term monitoring of physiological signals," *Med. Biol. Eng. Comput.*, vol. 42, no. 3, pp. 419–427, 2004.
[33] B. Güntekin and E. Başar, "A review of brain oscillations in perception of faces and emotional pictures," *Neuropsychologia*, vol. 58, no. 1, pp. 33–51, May 2014.
[34] M. Jerram, A. Lee, A. Negreira, and D. Gansler, "The neural correlates of the dominance dimension of emotion," *Psychiatry Res., Neuroimaging*, vol. 221, no. 2, pp. 135–141, Feb. 2014.
[35] D. Kukolja, S. Popoviĉ, M. Horvat, B. Kovač, and K. Ćosić, "Comparative analysis of emotion estimation methods based on physiological measurements for real-time applications," *Int. J. Hum.-Comput. Stud.*, vol. 72, nos. 10–11, pp. 717–727, Oct./Nov. 2014.
[36] S. Migliore *et al.*, "Emotional processing in RRMS patients: Dissociation between behavioural and neurophysiological response," *Multiple Sclerosis Related Disorders*, vol. 27, pp. 344–349, Jan. 2019.
[37] V. D. Calhoun and T. Adali, "Unmixing fMRI with independent component analysis," *IEEE Eng. Med. Biol. Mag.*, vol. 25, no. 2, pp. 79–90, Apr. 2006.
[38] E. L. Dennis and P. M. Thompson, "Functional brain connectivity using fMRI in aging and Alzheimer's disease," *Neuropsychol. Rev.*, vol. 24, no. 1, pp. 49–62, Mar. 2014.
[39] C. Vargas, C. López-Jaramillo, and E. Vieta, "A systematic literature review of resting state network—Functional MRI in bipolar disorder," *J. Affect. Disorders*, vol. 150, no. 3, pp. 727–735, Sep. 2013.

BO-LIN JIAN received the B.S. degree from the Department of Electrical Engineering, National Formosa University, in 2009, the M.S. degree in materials science and engineering from the National Taiwan University of Science and Technology, in 2011, and the Ph.D. degree from the Department of Aeronautics and Astronautics, National Cheng Kung University, in 2017.

He is currently an Assistant Professor with the Department of Electrical Engineering, National Chin-Yi University of Technology, Taichung, Taiwan. His current research interests include signal and image processing, machine learning, and control systems.

CHIEH-LI CHEN (M'01) received the B.S. degree in mechanical engineering from National Taiwan University, Taipei, Taiwan, in 1983, and the M.S. and Ph.D. degrees in control engineering from the University of Manchester Institute of Science and Technology (UMIST), Manchester, U.K., in 1987 and 1989, respectively. He is currently a Professor with the Department of Aeronautics and Astronautics, National Cheng Kung University, Tainan, Taiwan, where he currently teaches in the areas of automatic control and machine vision. His research interests include automation, optimization, nonlinear dynamics, robust control, vibration and energy system management, and machine vision.

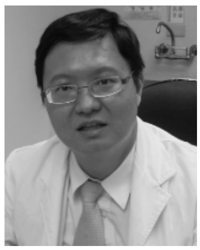

MIN-WEI HUANG received the M.S. and Ph.D. degrees from the Department of Biomedical Engineering, National Cheng Kung University. He is currently a Medical Doctor with the National Yang-Ming University. He is also the Deputy Superintendent with the Department of Psychiatry, Taichung Veterans General Hospital, Chiayi Branch.

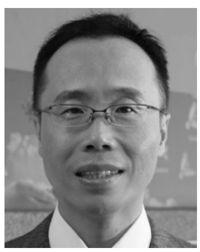

HER-TERNG YAU received the B.S. degree in mechanical engineering from the National Chung Hsing University, Taichung, Taiwan, in 1994, and the M.S. and Ph.D. degrees in mechanical engineering from the National Cheng Kung University, Tainan, Taiwan, in 1996 and 2000, respectively. He is currently a Professor with the Department of Electrical Engineering, National Chin-Yi University of Technology, Taichung. His research interests include energy converter control, system control of mechatronics, nonlinear system analysis, and control. He has authored more than 150 research articles on a wide variety of topics in mechanical and electrical engineering.